16th European Signal Processing Conference (EUSIPCO 2008), Lausanne, Switzerland, August 25-29, 2008, copyright by EURASIP

RELAXING THE HALF-WAVELENGTH CONDITION FOR ESTIMATING SIGNAL AOA AT A LINE OF SENSORS

Mohamed H. El-Shafey, Tareq Abdul-Rahman, and Yasser H. Dakroury

Department of Computer & Systems Engineering, Ain Shams University
1 Abdu Pacha Abbasya, 11517, Cairo, Egypt
phone: +202 22729507, fax: +202 26850617, email: elshafey@gmail.com

ABSTRACT

This paper introduces an estimation technique for the angle of arrival (AOA) of incident signal on a line of sensors from the differences of the signal phases at different sensors. Unlike known techniques, the distances separating neighbouring sensors may exceed half the wavelength 'lambda' of the incident signal. The proposed technique assumes estimating the continuous frequency (in rad/sec) and the phase of the sinusoids in the signal at each sensor in a previous step. Knowing the continuous frequency, and consequently the wavelength, it becomes possible to detect the occurrence of multiple complete wave cycles between sensors, thus relaxing the half-wavelength condition. To be able to detect multiple cycles, the technique assumes one of two conditions: 1- the signal contains at least two frequencies, and if not 2- there are at least three unequally spaced sensors. A maximum limit, greater than half the wavelength, is derived for the sensors spacing while still being able to resolve the ambiguity caused by the possibility of multiple cycles. Numerical results show good statistical behaviour of the technique.

1. INTRODUCTION

The development of smart antennas and land cellular position location has boosted the research in estimating the angle of arrival (AOA) of signals at the receivers. The angle of arrival (AOA), time of arrival (TOA), and time difference of arrival (TDOA) techniques have been proposed for providing location services in wireless networks. The AOA, TOA, TDOA, or a combination [1]-[5], at two, three or more receiver sites are commonly used in surveillance applications to accurately locate an aircraft, vehicle, or stationary emitter. Measuring AOA at the base station from a mobile hand ser can serve to increase downlink capacity via beamforming.

The simplest way to estimate the TOA or TDOA is through correlating the received signal at each receiving site with a local signal such that the largest peak represent the time of flight to each individual receiver.

The AOA on a sensor of arrays is determined by measuring the TDOA at individual elements of the array. Sometimes the TDOA measurement is made by measuring the difference in received phase at each element. Determining the time difference from the phase difference mandates placing the array elements at distances less than half the wavelength of the incident signal.

Subspace-based algorithms [6]-[9], known of having fine resolution, represent a different class of AOA estimation algorithms based on eigenvalue decomposition of the correlation matrix of signal samples, or the singular value decomposition of the matrix of signal samples to estimate the signal and noise subspaces. The data used are spatial samples of the signal taken at a number of sensors in an array. It is generally assumed that the number of sensors is greater than the number of impinging signals. Again the half wavelength rule should be observed. Of all subspace algorithms, the multiple signal classification (MUSIC) probably is the most popular. It estimates the AOA of signals based on the orthogonal property of the noise subspace eigenvectors and steering vectors [10]-[12]. The AOAs are determined by searching for the peaks of a pseudo-spectrum function; a problem similar to nonadaptive spectral estimation. Usually a methodology that results directly in numeric values is always preferable; this is where Root-MUSIC comes in. The AOA estimates are obtained by solving for the roots of a polynomial instead of searching for maxima. Estimation of Signal Parameters using Rotational In-variance Technique (ESPRIT) [13] is another parametric estimation technique, based on the fact that the steering vector at the elements has a constant phase shift from the adjacent elements. The Matrix Pencil [14] is similar to ESPRIT but it works directly with the data observation matrix instead of correlation matrix, thus saving some computations.

The AOA estimation technique in this paper can be regarded as a member of the class of TOA, TDOA, and phase difference of arrival. The signal TDOA is determined from the difference in signal phase at different sensors spaced by large distances breaking the half-wavelength limit. The technique assumes that the wavelengths of the incident signals are known, so that it can detect the occurrence of complete cycles between sensors. If the wavelengths are not known beforehand, they can be determined from estimates of the continuous frequencies as in [15],[16]. The rest of the paper is organized as follows: The AOA estimation problem is formulated in section 2. The technique to detect the occurrence of whole cycles between sensors is presented in section 3 with a proof of the limit on the sensors' maximum interspacing to guarantee the success of the technique. Numerical results are given in section 4. The paper concludes by commenting on the theoretical and numerical results in section 5.

2. PROBLEM ANALYSIS

In this work we assume a number of sensors assembled on a straight line receiving a signal from a far field emitter. It is required to estimate the AOA given the phase of the signal measured at each sensor knowing the frequencies, or equivalently the wavelengths, of the sinusoidal components of the signal s given by

$$s(t,x) = Ae^{j(2\pi ft - 2\pi\frac{x}{\lambda} + \phi_0)}. \quad (1)$$

In (1) f is the sinusoid's frequency in Hertz, A is its amplitude, λ is its wavelength, x is the distance along the direction of propagation, and ϕ_0 is the phase at $t = x = 0$. The information about the AOA of the signal at the sensors array is contained in the phases of the sinusoids at each sensor, as the signal arrives at each sensor at different phase depending on the time of arrival at that sensor,

which in turn is a function of the AOA. Let $\Phi(t,x)$ denotes actual signal phase at time t and distance x, then

$$\Phi(t,x) = 2\pi ft - 2\pi\frac{x}{\lambda} + \phi_0 \quad (2)$$

From (2), the difference in the actual signal phase between a point at arbitrary distance x and a reference point $x = 0$ at time zero, $\Delta\Phi(0,x) \equiv \Phi(0,x) - \Phi(0,0)$, is given in terms of x as

$$\Delta\Phi(0,x) = -2\pi\frac{x}{\lambda} = -\beta x \quad (3)$$

where β is the angular wavenumber. It would have been straightforward to obtain x from the phase difference in (3) if the actual phases of the signal could be determined from measurements. Unfortunately, the phase of the signal at any time instant and distance as estimated from the signal measurements appears inside the period $]-\pi \quad \pi]$, so all values of the actual phase outside that period are folded inside. This fact leads to the definition of what we may call the apparent phase $\phi(0,x)$

$$\phi(0,x) \equiv \Phi(0,x) - 2\pi i \quad : (2i-1)\pi \le \Phi(0,x) < (2i+1)\pi \quad (4)$$

A plot of the apparent versus the actual phase would be a saw-tooth waveform with odd symmetry, period 2π, and peak-to-peak value 2π. Rearranging terms in the inequalities in (4) gives i as the integer satisfying $\frac{\Phi(0,x)}{2\pi} - \frac{1}{2} < i \le \frac{\Phi(0,x)}{2\pi} + \frac{1}{2}$, i.e. i is the *floor* of $\frac{\Phi(0,x)}{2\pi} + \frac{1}{2}$. The relation between the apparent phase and the distance x is obtained by substituting for $\Phi(0,x)$ from (2) into (4):

$$\phi(0,x) = -2\pi\frac{x}{\lambda} + \phi_0 - 2\pi i \quad : i = fl(-\frac{x}{\lambda} + \frac{\phi_0}{2\pi} + \frac{1}{2}) \quad (5)$$

where fl(.) is the *floor* of (.).

Defining the normalized phase ϕ_n as the apparent phase ϕ divided by 2π, and the normalized distance z as the distance x divided by λ, we may rewrite (5) after replacing i by $k = -i$ as

$$\phi_n(0,z) = -z + \phi_{0n} + k \quad : k = fl(z - \phi_{0n} - \tfrac{1}{2}) \quad (6)$$

where ϕ_{0n} is ϕ_0 divided by 2π. From (6) we can obtain an equation like (3) relating the apparent phase difference and the distance in normalized form as:

$$\Delta\phi_n(0,z) \equiv \phi_n(0,z) - \phi_{0n} = -z + k \quad : k = fl(z - \phi_{0n} - \tfrac{1}{2})$$

which by dropping the time and distance arguments, for the sake of brevity, becomes

$$\Delta\phi_n = -z + k \quad : k = fl(z - \phi_{0n} - \tfrac{1}{2}) \quad (7)$$

Equation (7) illustrates that for every single value of $\Delta\phi_n$ we have multiple values for z, i.e. it is not possible to determine z for a given $\Delta\phi_n$ unless we restrict z to a single period of the waveform. Therefore, in order to guarantee a single-valued mapping $\Delta\phi_n :\rightarrow z$ symmetrically around $z = 0$ we should restrict z to

$$|z| < \tfrac{1}{2} \quad \leftrightarrow \quad |x| < \frac{\lambda}{2} \quad (8)$$

To illustrate the relation between the phase difference at different sensors and the signal AOA at the sensors consider two sensors S_0 and S hit by a planar waveform. Let's take $x = 0$ at S_0, considering it as the reference to measuring the distance along the direction of propagation. The distance x is related to the distance d separating the sensors and the AOA $\theta \in [-\frac{\pi}{2} \quad \frac{\pi}{2}]$ by $x = d \times \sin(\theta)$, therefore from the condition (8) we get: $d|\sin(\theta)| < \frac{\lambda}{2}$. Since $|\sin(\theta)| \le 1$ for $\theta \in [-\frac{\pi}{2} \quad \frac{\pi}{2}]$, then the condition on d becomes

$$d < \frac{\lambda}{2} \quad (9)$$

The condition (9) is a well known fact in spatial sampling of signals. If d exceeds half the wavelength, the unique mapping $\phi_n :\rightarrow z$ does not hold and we get many values of z, and θ, '*spatial aliases*', corresponding to a single value of the phase difference. If we use large d violating (9) we should restrict the range of estimating the AOA to a smaller value: $|\theta| < \sin^{-1}(\frac{\lambda}{2d}) < \frac{\pi}{2}$.

In what follows we present two anti-aliasing techniques to relax the spatial sampling limit (9). The first technique assumes having only two sensors. In this case we assume the signal contains at least two frequencies. The second technique works in case we have a single frequency, and it relies on nonuniform spatial sampling made by three unequally spaced sensors. Both techniques assume that the true continuous frequencies (not aliases) and consequently the correct wavelengths in the signal are known or estimated in a previous step using e.g. [15]. Under this assumption, we present two antialiasing methods to determine the number of complete cycles possibly made by individual frequency components, thus resolving the ambiguity of determining z, and accordingly θ, from the apparent phase difference. The antialiasing techniques are presented in the following section with a derivation of the maximum allowed sensor spacing.

3. ANTIALIASING TECHNIQUES

Let's define the dependent variable $z' = (1+r)z$, where r is a positive constant less than unity: $0 < r < 1$ which makes $z' > z$ with the same sign. Being a scaled value of the normalized distance z, the variable z' too can be regarded as normalized distance obtained for another wavelength λ' or another sensor at d'. Similar to the normalized phase difference in (7), the normalized phase difference corresponding to z' is a saw-tooth waveform with segments of straight lines numbered by the integer k':

$$\Delta\phi'_n = -z' + k' \quad : k' = fl(z' - \phi'_{0n} + \frac{1}{2(1+r)}) \quad (10)$$

Substituting for z' in (10) in terms of z and r and rearranging we obtain

$$\Delta\phi'_n = -(1+r)z + k' \quad : k' = fl(z + rz - \phi'_{0n} + \frac{1}{2(1+r)}) \quad (11)$$

As compared to $\Delta\phi_n$, $\Delta\phi'_n$ differs in: period: $\frac{1}{1+r} < 1$, slope of line segments: $-(1+r)$, and mean value: ϕ'_{0n}, but both have unity peak-to-peak value. Plots of $\Delta\phi_n$ and $\Delta\phi'_n$ are shown in Fig. 1 (a) and (b) for $r = \frac{1}{5}$ and normalized initial phases $\phi_{0n} = 0.1$, and $\phi'_{0n} = 0.15$ (picked randomly). Figure 1 (c) is the phase difference $\delta\phi_n$ defined as

$$\delta\phi_n \equiv \Delta\phi'_n - \Delta\phi_n = -rz + (k' - k) \quad (12)$$

The plot of $\delta\phi_n$ shows a five-times extension of the period of single-valued mapping $\delta\phi_n :\rightarrow z$; $]-2.5 \quad 2.5]$, as compared to the unity period of single-valued mapping $\Delta\phi_n :\rightarrow z$; $]-0.5 \quad 0.5]$.

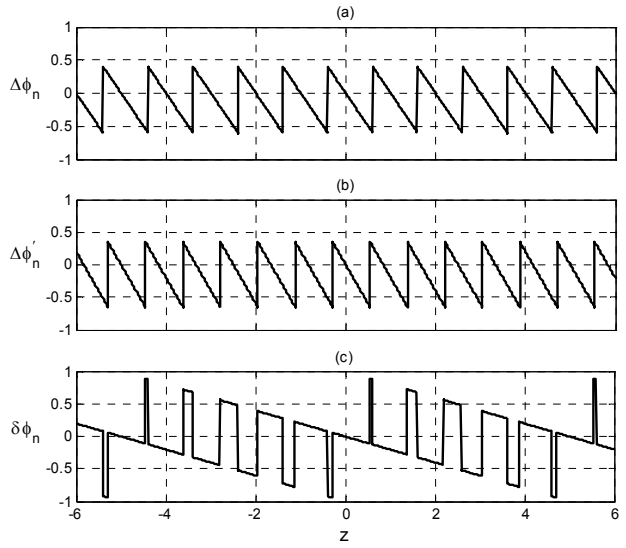

Fig. 1. Apparent normalized phase difference versus normalized distance for $r = \frac{1}{5}$

It is required to establish a limit on z where the single-valued mapping $\delta\phi_n :\rightarrow z$ holds. This limit is given by the following statement:

The mapping $\delta\phi_n :\rightarrow z$, *the inverse of* (12), *is single valued inside the period* $|z| < \frac{1}{2r}$.

Proof:

It is sufficient to prove that the parallel straight lines $\ell_m = -rz + m$ for any integer m do not overlap horizontally inside the specified period. We seek the period of z where for any integer $m' \neq m$ the following two conditions are met:

$$\text{If } m' > m \text{ then } \max(\ell_m) < \min(\ell_{m'}) \quad (c1)$$

$$\text{If } m' < m \text{ then } \min(\ell_m) > \max(\ell_{m'}) \quad (c2)$$

Let $P = [z_{min} \quad z_{max}]$, then inside P we may specify two cases:

1- $m' > m$: $\max(\ell_m) = -rz_{min} + m$, $\min(\ell_{m'}) = -rz_{max} + m'$.

Then in order to satisfy (c1) we should have:

$\max(\ell_m) - \min(\ell_{m'}) = rz_{max} - rz_{min} + m - m' < 0$, i.e.

$$z_{max} - z_{min} < \frac{m'-m}{r}$$

but the minimum possible value of $m'-m$ is 1, so to guarantee the last inequality we should have

$$z_{max} - z_{min} < \frac{1}{r} \quad (c3)$$

2- $m' < m$: $\min(\ell_m) = -rz_{max} + m$, $\max(\ell_{m'}) = -rz_{min} + m'$.

Then in order to satisfy (c2) we should have:

$\min(\ell_m) - \max(\ell_{m'}) = -rz_{max} + rz_{min} + m - m' > 0$, i.e.

$$z_{max} - z_{min} < \frac{m-m'}{r}$$

Again the minimum possible value of $m-m'$ is 1, so to guarantee the above inequality, we should have condition (c3) satisfied. In order to make P symmetrical around zero we may choose $z_{max} = -z_{min} = z_m$, hence we obtain $z_m < \frac{1}{2r}$ leading to $-\frac{1}{2r} < z < \frac{1}{2r}$ which completes the proof.

We have $z = \frac{x}{\lambda} = \frac{d\sin(\theta)}{\lambda}$ then the extreme values of z correspond to $\sin(\theta) = \pm 1 : |z| \leq \frac{d}{\lambda}$ leading to $\frac{d}{\lambda} < \frac{1}{2r}$ so the new limit on the maximum sensors' interspacing is:

$$d < \frac{\lambda}{2r} \quad (13)$$

and because $r < 1$, this new limit is larger than the standard limit (9) by a factor of $\frac{1}{r}$.

The determination of the AOA θ from the phase differences $\Delta\phi_n$ and $\Delta\phi'_n$ takes the following steps:

1- Determine the set z_1 of all possible values of z from $\Delta\phi_n$ using (7)

2- Determine the set z2 of all possible values of z from $\Delta\phi'_n$ using (11)

3- Determine k and k' corresponding to those values from z_1 and z_2 closest to each other: $[\hat{k}, \hat{k}'] = \arg\min_{[k,k']} (z_1(k) - z_2(k'))^2$

4- Obtain two estimates of the AOA as $\hat{\theta}_1 = \sin^{-1}(\frac{\lambda z_1(\hat{k})}{d})$ and $\hat{\theta}_2 = \sin^{-1}(\frac{\lambda z_2(\hat{k}')}{d})$

5- Obtain the estimate of θ as the mean value of $\hat{\theta}_1$ and $\hat{\theta}_2$.

The search for the minimum in step 3 requires evaluating $(z_1 - z_2)^2$ for all possible combinations of k and k' which are at least equal to k^2 since $k' \geq k$. To reduce the number of computations we make use of (12) to limit the number of possible k' for a given k. From (12) we have $k' - k = \delta\phi_n + rz$, but $-2 < \delta\phi_n < 2$ and $-\frac{1}{2} < rz < \frac{1}{2}$, then $k' - k$ is limited by $-2\frac{1}{2} < k' - k < 2\frac{1}{2}$, i.e. there is only five possible values of $k' - k$; $-2, -1$, 0, 1, and 2, making the required number of computations $5k < k^2$ in case $k > 5$.

4. NUMERICAL EXAMPLES

***A- Antialiasing by two frequencies: same d, different f*:**

In this section we assume the distance d exceeds the spatial sampling limit (9), and the signal contains two frequencies f and f' such that $f' = (1 + r)f$. According to (13), the positive r should be less than unity in order to let d exceed the standard limit of half the wavelength, so f' should satisfy $f < f' < 2f$.

Numerical values:

Assuming a sound wave ($c = 34400 cm/sec$) with the following parameters:

$f = 5kHz$, $f' = 6kHz$, $r = \frac{1}{5}$, $\lambda = 6.88cm$, so $\lambda' = 5.7333cm$.

According to (13), the distance separating the sensors should be limited by $d < \frac{\lambda}{2r} = \frac{5}{2}\lambda$, so we take $d = 2.4\lambda$. We assume that the phase of each sinusoid at each sensor is estimated, and that the estimate is deviated from the true phase by some error which we assume to be uniformly distributed over the period $\sigma]-\pi \quad \pi]$ where the value of σ is chosen to reflect the confidence in the phase estimate: the larger σ the less confidence we have in the estimate.

Accordingly, the normalized phase error is uniformly distributed over the period $\sigma\,]-0.5 \quad 0.5]$.

Case 1: Low estimation error ($\sigma = \sqrt{0.001}$)

The estimation errors in both ϕ_n and ϕ'_n at this value of σ are uniformly distributed over the period $]-5.69^o \quad 5.69^o]$, and consequently the distributions of both $\Delta\phi$ and $\Delta\phi'$ take triangular shape over twice that period: $]-11.38^o \quad 11.38^o]$ as can be seen in Fig. 2-a. The plots in Fig. 2 are approximation of the probability density functions (pdf) of the random errors calculated as the relative frequency of occurrence of the error over every small interval of the abscissa in ten thousand trials. The abscissa is divided into 21 equal intervals $\Delta_k, k = -10,\ldots,10$ and the number of times the error occurs inside Δ_k is calculated and divided by the total number of trials (10,000). The plots correspond to three values of AOA: $\theta = [-10^o \quad 0^o \quad 60^o]$: a shallow, zero, and a wide angle. In Fig. 2-a we have two plots of the error in $\Delta\phi_n$ and $\Delta\phi'_n$ for each case of θ. (Note that the six plots approximate the same triangular shape). Plots of the approximated pdf of the error in estimating θ for the three cases are shown Fig. 2-b. The plots show that the estimation error pdf is symmetric around a peak value at zero which means that the estimates of θ are unbiased and the correct value is the most probable. The plots also show that the values of the estimation error variance are low (less than 1^o).

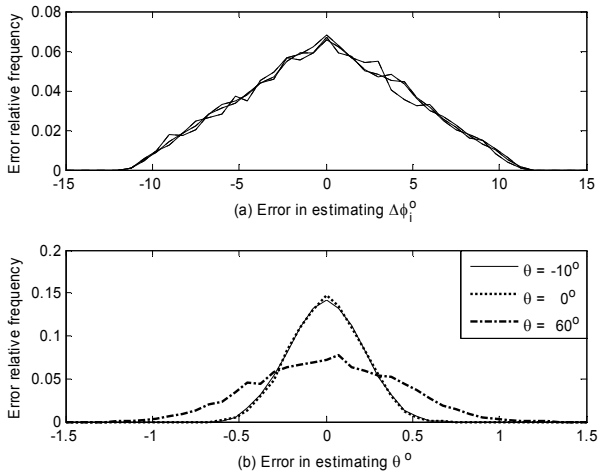

Fig. 2. Relative frequency of occurrence of estimation errors for three different AOA (Low σ)

To show the effect of the value of d on the estimates of θ, the estimation program was run with all parameters kept the same except for the sensors' distance which is reduced to $d = \frac{\lambda}{2}$; the standard antialiasing limit. In Fig. 3 the plots of the approximate pdfs of the estimation errors show larger estimation variances as compared to the case of $d = 2.4\lambda$ in Fig. 2 which means that by increasing d we obtain more consistent estimates. The reason behind improved estimates is that by increasing d with respect to the wavelength λ, the sensitivity of the phase differences $\Delta\phi$ and $\Delta\phi'$ to changes in θ increases as can be seen from (3) where $x = d \times \sin(\theta)$.

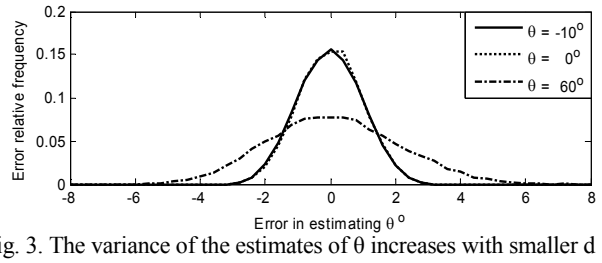

Fig. 3. The variance of the estimates of θ increases with smaller d

Case 2: large estimation error ($\sigma = 0.1$)

The estimation errors in both ϕ_n and ϕ'_n, in this case, are uniformly distributed over the period $]-18^o \quad 18^o]$; more than three times the period in Case 1. Hence, the distributions of both $\Delta\phi_n$ and $\Delta\phi'_n$ take triangular-shape over $]-36^o \quad 36^o]$ and they almost coincide as can be seen in Fig. 4-a.

The plot of the approximate pdf of the estimation error in θ for $\theta = 10^o$ is in Fig. 4-b which shows that the correct value is the most probable estimate and the error pdf is symmetric about zero with small variance. However the plot reveals the possibility of estimate outliers which are seen on the sides of the plot. The positions of the outliers in the plot are determined by an error of a whole cycle in estimating both $\Delta\phi_n$ and $\Delta\phi'_n$ as can be seen from the following analysis.

The correct value of x corresponding to $\theta = 10^o$ is given by $x = d\sin(10^o) = 2.4\lambda\sin(10^o) = 0.4168\lambda$. An error of a whole cycle in the phase difference estimate corresponds to a complete wavelength in the estimate of x, i.e. $\tilde{x} = x \pm \lambda$ and $\tilde{x}' = x \pm \lambda'$ leading to the incorrect estimates of $\sin(\theta)$ as:

$$\sin(\hat{\theta}_1) = \frac{x \pm \lambda}{d} = \frac{0.4168\lambda \pm \lambda}{2.4\lambda} \text{ giving } \tilde{\theta}_1 \in \{36.18^o \quad -14.1^o\}$$

$$\sin(\tilde{\theta}_2) = \frac{x \pm \lambda'}{d} = \frac{0.4168\lambda \pm \lambda/(1.2)}{2.4\lambda}, \text{ so } \tilde{\theta}_2 \in \{31.4^o \quad -10^o\}$$

The mean values of the estimates $\hat{\theta}_1$ and $\hat{\theta}_2$ are $\tilde{\theta} \in \{33.79^o \quad -12.03^o\}$ which means that the estimation error is $\{23.79^o \quad -22.03^o\}$ conforming with the plot.

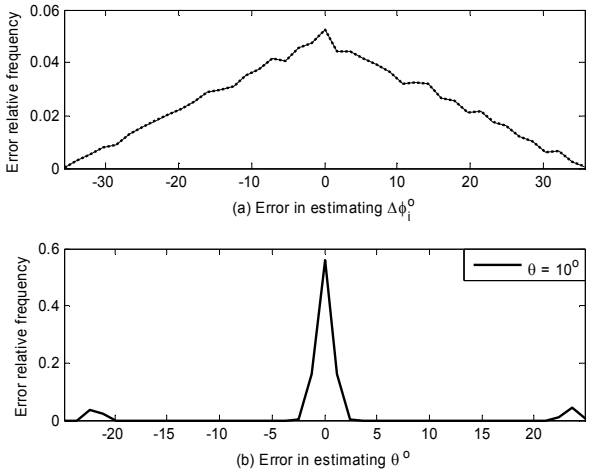

Fig. 4. Large errors in estimating the phase difference result in outliers in the estimate of AOA (High σ)

***B- Antialiasing by two distances: same f, different d*:**
Here we assume having three sensors S_0, S_1, and S_2.The distance between S_0 and S_1 is d, and the distance between S_0 and S_2 is $d' = (1+r)d$. Since r satisfies $0 < r < 1$, then the condition on d' is $d < d' < 2d$.

Numerical values:

$f = 5\text{kHz}$, $\lambda = 6.88\text{cm}$, $r = \frac{1}{5}$, $d = 2\lambda$, so $d' = 2.4\lambda$.

Similar to section *A* we study two cases with low and high phase estimation errors. The results obtained are quite similar to those obtained in section *A*.

Case 1: Low estimation error ($\sigma = \sqrt{0.001}$)

The approximate pdf of the error in estimating $\Delta\phi_n$ and $\Delta\phi'_n$ should be the same as in Fig. 2-a. The plots of the pdf of the error in estimating three cases of the AOA $\theta = [-10^o \quad 0^o \quad 60^o]$ in Fig. 5 show unbiased low-variance estimates; same as in Fig. 2-b.

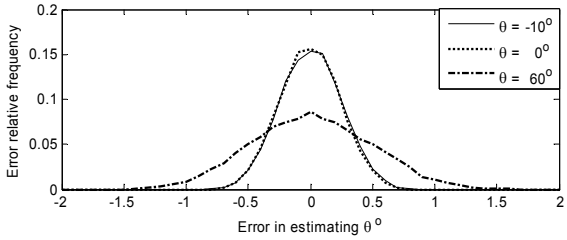

Fig. 5. Relative frequency of occurrence of estimation errors for three different AOA (Low σ)

Case 2: large estimation error ($\sigma = 0.1$)

By increasing the error levels in the estimates of $\Delta\phi_n$ and $\Delta\phi'_n$, the outliers in θ estimates appear (see Fig. 6 where $\theta = 10^o$). The outliers are the result of an error of one wavelength error in evaluating x. The positions of the outliers in this case are obtained as the mean values of $\tilde{\theta}_1$ and $\tilde{\theta}_2$ determined by

$$\sin(\tilde{\theta}_1) = \frac{x \pm \lambda}{d} = \frac{0.4168\lambda \pm \lambda}{2\lambda}, \text{ giving } \tilde{\theta}_1 \in \{36.18^o \quad -14.06^o\}$$

$$\sin(\tilde{\theta}_2) = \frac{x' \pm \lambda}{d'} = \frac{0..3473\lambda \pm \lambda}{2.4\lambda}, \text{ giving } \tilde{\theta}_2 \in \{42.35^o \quad -19.05^o\}$$

The mean values of the estimates $\hat{\theta}_1$ and $\hat{\theta}_2$ are $\tilde{\theta} \in \{39.26^o \quad -16.56^o\}$ which means that the estimation error is $\{29.26^o \quad -26.56^o\}$ conforming with the plot.

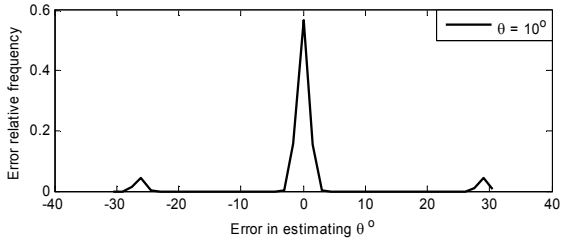

Fig. 6. Large errors in estimating the phase difference result in outliers in the estimate of AOA (High σ)

5. CONCLUSION

A technique is introduced for estimating the AOA from the phase difference at sensors spaced by more than half the wavelength. The technique resolves the ambiguity of mapping phase difference to time difference by assuming multiple sinusoids in the signal, or by utilizing multiple unequally-spaced sensors. Better estimates are attained as sensors with larger interspacing exhibit higher sensitivity to the AOA for the same wavelength. Alternatively, the same sensor array would exhibit higher sensitivity for shorter wavelengths. It is shown that the mapping of the phase difference to time difference in order to estimate the AOA introduces no bias to the estimate provided that the error in the phase difference estimation algorithm is itself unbiased and uniformly distributed. As the error in the phase difference estimates increases it becomes possible to have outliers in the estimate of the AOA corresponding to a complete-cycle error in the phase difference (a whole wavelength error in the distance).

REFERENCES

[1] W. Li, P. Liu, "3D AOA/TDOA emitter location by integrated passive radar/GPS/INS systems," in *Proc. of 2005 IEEE International Workshop on VLSI Design and Video Technology*, 2005, pp. 121-124

[2] S. Venkatraman, and J. Caffery, Jr., "Hybrid TOA/AOA techniques for mobile location in non-line-of-sight environments," *IEEE Wireless Communications and Networking Conference*, WCNC. 2004, Vol. 1, pp. 274-278

[3] F. Mrabtia, M. Elhajjamib, and M. Zouaka, "Performance analysis of joint DOA/TOA estimator," *Signal Processing* 84, 1359 – 1365, 2004

[4] N. J. Thomas, D. G. M. Cruickshank, and D. I. Laurenson, "Performance of a TDOA-AOA hybrid mobile location system," *Second International Conference on 3G Mobile Communication Technologies*, 2001. (Conf. Publ. No. 477), pp. 216-220

[5] Y. W. Lee, J. S. Kim, and W. G. Chung , "Position location error analysis by AOA and TDOA using a common channel model for CDMA cellular environments," in *Proc. IEEE 51st Vehicular Technology*, Tokyo. 2000, Vol. 3, pp. 2394-2397

[6] A. Tanaka, H, Imai, and M. Miyakoshi, "A Unified Framework of Subspace Identification for D.O.A. Estimation," *IEICI Transactions on Fundamentals of Electronics, Communications, and Computer Sciences*, Vol. E90-A(2), pp. 419-428, 2007

[7] H. Abeida, J. Delmas, "Efficiency of subspace-based DOA estimators," *Signal Processing* 87, pp. 2075–2084, 2007

[8] Y. Wua,_, L. Mab, C. Houa, G. Zhangc, and J, Lic, "Subspace-based method for joint range and DOA estimation of multiple near-field sources," *Signal Processing* 86, pp. 2129–2133, 2006

[9] A. Olfat, S. Nader-Esfahani, "A new signal subspace processing for DOA estimation," *Signal Processing* 84, pp. 721 – 728, 2004

[10] Jen-Der Lin, Wen-Hsien Fang, Yung-Yi Wang, and Jiunn-Tsair Chen, "FSF MUSIC for joint DOA and frequency estimation and its performance analysis," *IEEE Trans. on Signal Processing*, Vol. 54, No. 12, pp. 4529-4542, Dec. 2006

[11] S. Park, T. K. Sarkar, and R. D. Schneible, "Prevention of signal cancellation in an adaptive nulling problem," in *Proc. IEEE Radar Conf.*, 1997, pp. 191–195.

[12] K. Ichige, Y. Ishikawa, and H. Arai, "High Resolution DOA Estimation Using Second-Order Differential of MUSIC Spectrum," *IEICE Transactions on Fundamentals of Electronics, Communications and Computer Sciences*, Vol. E90-A(3), pp. 546-552, 2007

[13] S. Al-Jazzar, J. Caffery, Jr., "ESPRIT-based joint AOA/delay estimation for CDMA systems," in *IEEE Wireless Communications and Networking Conference*, WCNC 2004, Vol. 4, pp. 2244-2249

[14] J. Koh, D. Lim, and T. K. Sarkar, "DOA Estimation Using Matrix Pencil Method," *IEICE Transactions on Communications*, Vol. E87-B(5), pp. 1427-1429, 2004

[15] M. H. El-Shafey, "Effect of the sampling time on the accuracy of estimating the frequencies of multiple sinusoids," in *Proc. ICCES'06*, Cairo, Egypt, 2006, pp. 324-328

[16] M. H. El-Shafey, "Beating the Nyquist limit by utilizing samples of filtered sinusoids," in *Proc. ICEEC'04*, Cairo, Egypt, 2004, pp. 210-213